A computational study of the negative LiIn modified anode and its interaction with β-Li$_3$PS$_4$ solid-electrolyte for battery applications.

Naiara L. Marana[a], Fabrizio Silveri[a,b], Eduardo de Oliveira[c], Lorenzo Donà[a], Maddalena D'Amore[a], Eleonora Ascrizzi[a], Mauro Sgroi[a], Lorenzo Maschio[a], and Anna Maria Ferrari[a,*]

[a]Chemistry Department, University of Torino, via P.Giuria 5, 10125 Torino, Italy.

[b]Gemmate Technologies s.r.l., Buttigliera Alta, Torino 10090, Italy.

[c]Department of Analytical and Physical Chemistry, Universitat Jaume I, 12071 Castelló, Spain.
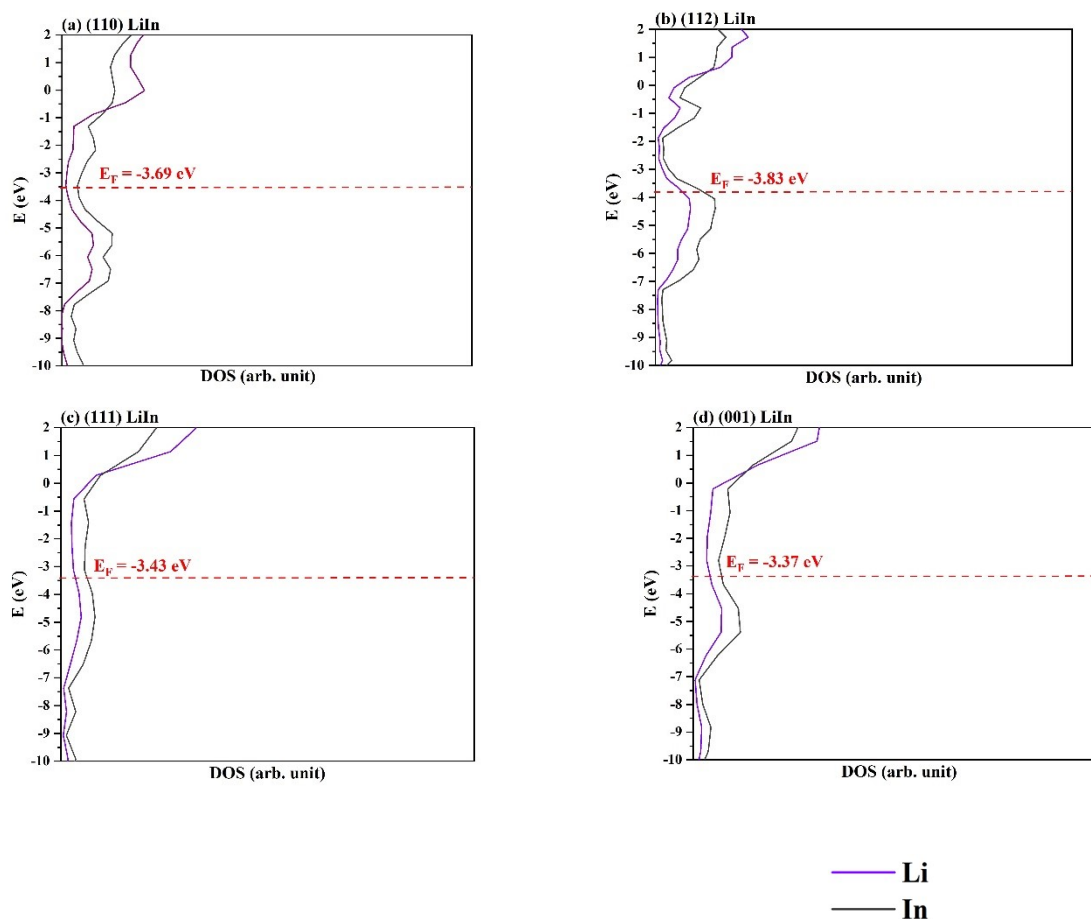
Supplementary Information

Figure S1: Projected density of states for the (a) (110), (b) (112), (c) (111), and (001) LiIn surfaces

Table S1: LiIn and LPS surfaces cell parameters ($a0$ and $b0$, in Å) and cell parameters (a and b, in Å) defining the coincidence cell used to form the interfaces. In parenthesis, the lattice mismatch percentage computed as:
$$\%_{xx(yy)} = \frac{a(b)_{LPS} - a(b)_{LiIn}}{a_{(b)LPS}}$$

Isolated sub-units		a_o	b_o
LPS(100)		6.24	8.08
LiIn(110)		3.30	4.67
LiIn(111)		4.67	4.67
LiIn(112)		4.67	5.72
Interface	Cell	a (%xx)	b (%yy)
(110)LiIn/(100)LPS	(2x2)LiIn/(1x1)LPS	6.60 (-5.77)	9.34 (-15.59)
(111)LiIn/(100)LPS	(4x2)LiIn/(3x1)LPS	18.68 (0.21)	8.08 (0.00)
(112)LiIn/(100)LPS	(4x3)LiIn/(3x2)LPS	18.68 (0.21)	17.15 (-6.13)

Table S2: Cohesive energy (E_{coh}, in eV/atom) for Li and In atoms in the LiIn, In, and Li bulk structures

	a_0	E_{coh}	Experimental[23]
LiIn$_{LiIn-bulk}$	6.74	-2.28	-
Li$_{Li-bulk}$	3.37	-1.51	-1.63
In$_{In-bulk}$	6.63	-2.30	-2.52

Determination of the zero of the electrostatic potential V as defined by the CRYSTAL code.

The work function is obtained as the difference between the energy of an electron at infinity and the Fermi energy: $E(\infty) - E_F$. To compute $E(\infty) - E_F$, knowledge of the electrostatic potential, which is determined from the charge density, and of the Fermi energy is necessary. Remember that $V = {E}/{e}$ (e is the electron charge).

In 2D slab models, the zero of the electrostatic potential V is defined by the CRYSTAL code in such a way that $V(\infty) = -V(-\infty)$, and the Fermi energy is then determined by the number of electrons. In the case of symmetrical arrangements of the slabs $V(\infty) = -V(-\infty) = 0$ holds, and the work function is $\phi = -E_F$.

In the general case of asymmetrical arrangements of the slabs, on one side of the slab (on the side pointing to $+\infty$, *defined as the left side for clarity*), $V(\infty) - E_F$ gives the left work function ϕ_{left}. $V(-\infty) - E_F$ corresponds to the work function of the other side of the slab ϕ_{right}. In these cases, the Fermi energy level is still reported as referred to the zero energy level assigned by the

CRYSTAL code, but a ΔV value is provided to quantify the energy difference between vacuum levels, $\Delta V = |V(\infty) - V(-\infty)|$.

In the same way, the proper alignememt of any energy level with the vacuum correlates HOMO or top of VB with the ionization potential and LUMO or bottom of CB with the electron affinity. Figure S2 illustrates the electrostatic potential calculation for selected cases: a) and b) the symmetric slab describing LPS and the LiIn (112) surface and c) an asymmetric case describing the LiIn (111) surfaces.
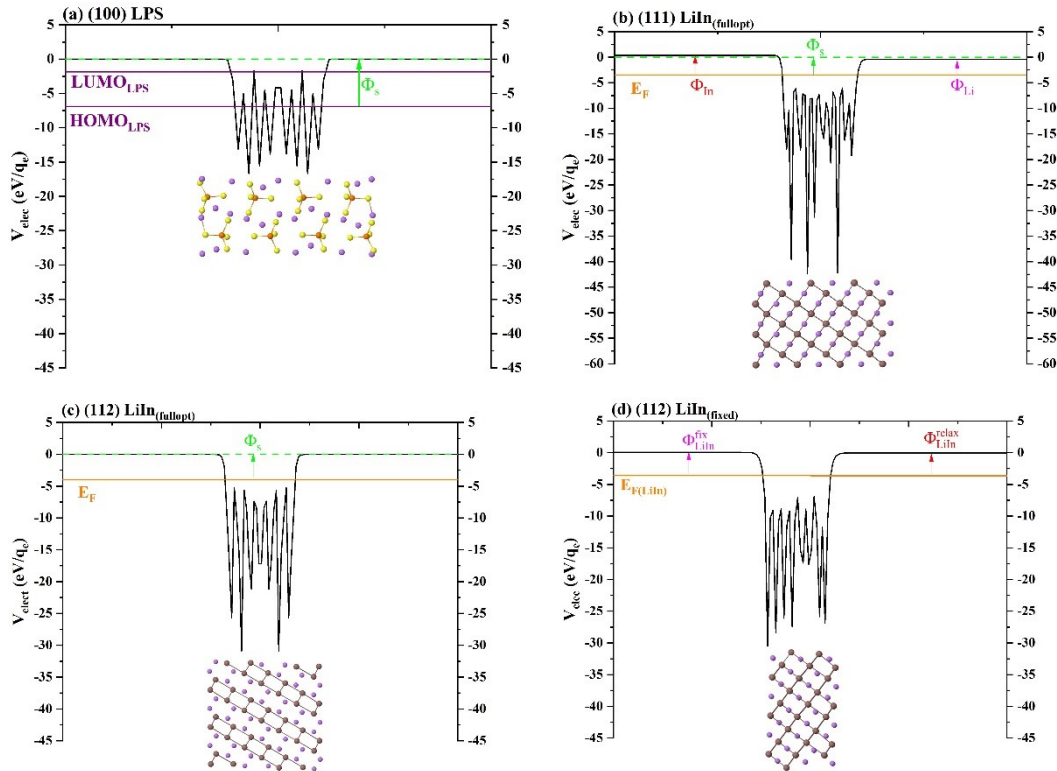

Figure S2: Electrostatic potential for the isolated surfaces (a) (100) LPS, (b) (111)LiIn, (c) (112)LiIn fully optimized, and (112)LiIn 3 layers fixed.

Thus for LiIn 112 $\phi_{left} = \phi_{right} = \phi_{(112)}$, but for LiIn 110 $\phi_{left} = \phi_{(111-In)}$ and $\phi_{right} = \phi_{(111-Li)}$. However, even in the case of symmetric slabs, some slab layers have been kept fixed at the bulk values during the geometric optimization of interfaces, introducing thus an asymmetry in the model slab (see Figure S2d). In this case, for the case reported in Figure S2d for the (112) surface, ϕ_{right} correspond to $\phi_{(112)}$, whereas

$\phi_{left} = \phi_{fixed}$ to a constrained bulk like surface that has any physical counterpart. Data for all surfaces of interest are collected in Table S3.

Table S3: Fermi energy (E_F, in eV), energy difference between vacuum levels (ΔV, in eV), surface work function (Φ, in eV), and the work function of each termination for the asymmetric surfaces (Φ_{left} and Φ_{right}, in eV)

LiIn(relaxed)	n_{layer}	E_F	ΔV	Φ	Φ_{left}	Φ_{right}
(110)	8	-3.69	0.00	3.69	-	-
(111)	8	-3.41	0.88	-	3.85_{In}	2.97_{Li}
(111)	20	-3.43	0.78	-	3.82_{In}	3.04_{Li}
(112)	8	-3.81	0.00	3.81	-	-
(112)	14	-3.83	0.00	3.83	-	-
LiIn(fixed)	n_{layer}	E_F	ΔV		$\phi_{left} = \phi_{fixed}$	$\phi_{right} = \phi_{LiIn}$
(110)	7	-3.93	0.13	-	4.06	**3.80**
(112)	8	-3.75	0.08	-	3.79	**3.71**
(111)-In	12	3.57	0.64	-	3.23	**3.91**
(111)-Li	12	-3.35	1.10	-	3.90	**2.80**
LPS surface	n_{layer}	*HOMO/LUMO*	ΔV		*IP*	*AE*
(100)	44	-7.02/-2.30	0.00	-	6.92	-2.30

Similar is the case of a LPS-LiIn interface. Figure S3 reports the V variation upon the LPS/LiIn(112) formation. In this case, ΔV is due to the dipole variation, charge redistribution, and bonds formation at the interface with respect to the non-interacting fragments. However in this case $\phi_{right} = \phi_{LPS-LiIn}$ that physically reproduces the work function variation when the interface is formed, but again $\phi_{left} = \phi_{fixed}$ has no physical counterpart. Table S4 reports the data for all the interfaces discussed in this paper. When calculated with respect to the positioning of $\phi_{LPS-LiIn}$, the energy levels of LPS CB and VB can be correlated with the electron affinity and the ionization potential of LPS in the heterosystems.
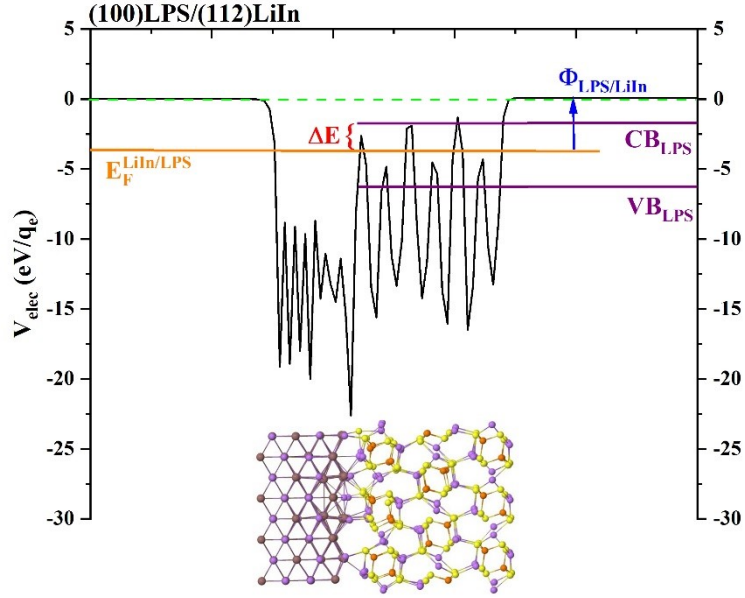
Figure S3: Electrostatic potential for the (100)LPS/(112)LiIn

Table S4: Fermi energy (E_F, in eV), energy difference between vacuum levels (ΔV, in eV), the interface work function of each termination, the LiIn fixed side (ϕ_{fixed}, in eV) and the interface LPS/LiIn side ($\phi_{LPS-LiIn}$, in eV)

LPS interfaces	E_F	ΔV	$\phi_{left} = \phi_{fixed}$	$\phi_{right} = \phi_{LPS-LiIn}$
(110)	-3.87	0.08	3.79	**3.85**
(112)	-3.78	0.031	3.75	**3.81**
(111)-In	-3.58	0.30	3.28	**3.88**
(111)-Li	-3.83	0.24	4.07	**3.60**

Table S5: Functional used, LiIn surface that made the interface with (100) LPS surface, adhesion energy (E_{adh}), basis set superposition error (E_{BSSE}), BSSE corrected adhesion energy (E_{adh}^{c}), in meVÅ^{-2}, and electron charge transfer (CT, in $10^{-3}|e|$Å^{-2}) for the analyzed interfaces (a positive value indicates an electron charge transfer from LiIn to LPS).

| Functional	LiIn surface	E_{adh}	E_{BSSE}	E_{adh}^{c}	CT
PBE0	(110)	-22.94	+10.84	-12.09	6.16
PBE0	(112)	-32.04	+14.12	-17.91	10.01
PBE0	(111)-In	-33.58	+16.59	-16.99	5.65
PBE0	(111)-Li	-28.04	+14.11	-13.91	3.51
MN15//PBE0	(110)	-37.34	+14.53	-22.81	6.99
MN15//PBE0	(112)	-48.43	+18.43	-30.01	9.27
MN15//PBE0	(111)-In	-47.62	+18.68	-28.93	11.26
MN15//PBE0	(111)-Li	-41.26	+16.08	-25.18	6.43
R2SCAN//PBE0	(110)	-25.65	+10.83	-14.82	6.25
R2SCAN//PBE0	(112)	-35.86	+14.02	-21.83	8.37
R2SCAN//PBE0	(111)-In	-35.64	+14.17	-21.47	9.57
R2SCAN//PBE0	(111)-Li	-29.44	+11.04	-18.40	6.72
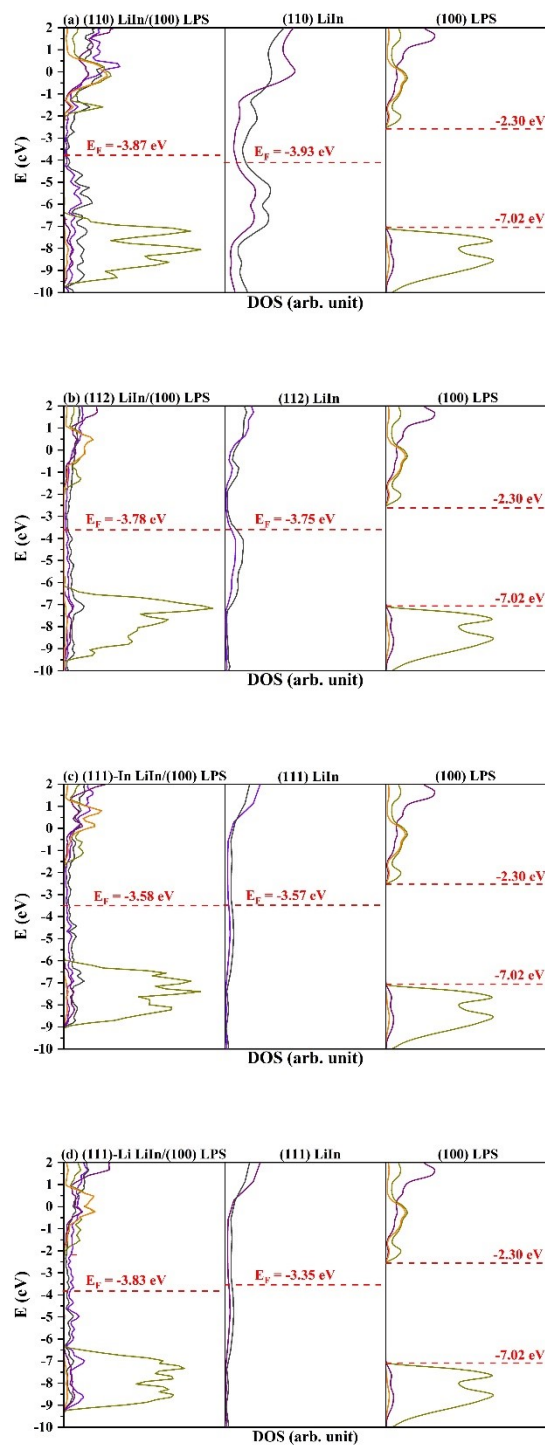
Figure S4: Projected density of states for the LiIn/LPS stable interfaces (a) (110) LiIn/(100)LPS, (b) (112) LiIn/(100)LPS, (c) (111)-In LiIn/(100)LPS, and (d) (111)-Li LiIn/(100)LPS